# Time-Domain Perturbational Analysis of Nonuniformly Coupled Transmission Lines

YING-CHING ERIC YANG, STUDENT MEMBER, IEEE, JIN AU KONG, FELLOW, IEEE, AND QIZHENG GU

*Abstract* — **A method of analyzing the time-domain behavior of a pair of nonuniformly coupled, dispersionless transmission lines is presented. The coupling coefficient of the system is assumed to be slowly varying with position. The set of coupled equations is transformed into a form for which the method of characteristics applies. Instead of numerically integrating the coupled equations, we decouple the equations by writing the solution in the form of a perturbational series. The resulting zeroth-order term corresponds to the inverse transform of the WKB approximation in the frequency domain, which contains only the wavefront and amplitude information. The higher order terms can be directly interpreted as reflections along the lines. Causality is satisfied to all orders. This method has the advantage of easier implementation, and is more versatile than frequency-domain methods as well as the brute-force numerical integration of the coupled partial differential equations.**

## I. Introduction

THE THEORY OF coupled transmission lines has been of continuous interest to both the microwave engineering and the power engineering communities. In microwave engineering, the energy exchange between coupled lines is of great concern and has been studied extensively [1]–[3], while in power engineering, the emphasis is on transient analysis [4], [5]. With the increasing applications of microstrip transmission lines in high-speed digital integrated circuits, the problem of eliminating crosstalks between adjacent lines becomes more important [6]–[9]. Because of the complex geometries, such as the presence of crossing wires at different heights [8], the coupling between two parallel lines is in general nonuniform. Accordingly, we need a more complete transient analysis of nonuniformly, as well as uniformly, coupled transmission lines.

Traditionally, the transient analysis of transmission lines was done in the frequency domain, and then inverse transformed to the time domain. Although straightforward, these methods were restricted in scope because of the difficulty involved in obtaining the solution analytically for general cases. There have been many articles treating transients on single, lossless, uniform transmission lines [10], [11], which can be easily extended to uniformly coupled multiline structures, and all the answers were obtained in closed form. Work has been done on transients involving resistive, or more generally, dispersive transmission lines [12–[15]. As for nonuniformly coupled lines, only a few special cases have been investigated. The WKB approximation, which is a standard technique for solving inhomogeneous wave equations, was widely used for analyzing single nonuniform transmission lines; however, it could get very complicated for higher order analysis when more lines are added. Direct time-domain formulations are usually set up for numerical integration, and the final forms are given by finite-difference equations [4]. Branin [16] introduced the method of characteristics to solve the transient problem of a single uniform, lossless line and constructed an equivalent circuit model to facilitate the implementation of his algorithm. Chang [17] generalized this concept to treat multiconductor lines. For nonuniformly coupled lines, general analytical schemes are not available. Although brute-force numerical integration lacked the direct link to physical interpretation as can be found in the case of uniformly coupled lines where the solution is written as the combination of several "modes" which stand for waves of constant amplitudes traveling in different directions with prescribed velocities, it has been adopted in some practical applications [18].

It is the purpose of this paper to show that by a suitable choice of transformation and a combination of the method of characteristics and perturbational series, we can obtain the transient response with sufficient accuracy from a set of iterative integration formulas which bear physical meanings. Each term in the perturbational series represents repetitive reflections along the lines due to nonuniform coupling. Moreover, for the case when the two lines are identical, the final solutions are given in closed form up to the first-order terms if the excitation is a unit step. The responses due to other types of input can be obtained by convolution. Therefore, in terms of efficiency, this method is superior to the usual frequency-domain methods, as well as the purely numerical integration approach in the time domain.

## II. Formulation of Coupled Transmission-Line Equations

Consider two nonuniformly coupled dispersionless transmission lines, as shown in Fig. 1, where a voltage source $e_s(t)$ is applied at line 1. The time-domain behavior of this system is governed by the following set of coupled equa-

Manuscript received January 16, 1985; revised June 10, 1985. This work was supported in part by the IBM Corporation, the Joint Services Electronics Programs under Contract DAAG29-83-00038408, and the Army Research Office under Contract DAAG29-85-K-0079.

The authors are with the Department of Electrical Engineering and Computer Science and the Research Laboratory of Electronics, Massachussets Institute of Technology, Cambridge, MA 02139.

0018-9480/85/1100-1120$01.00 ©1985 IEEE

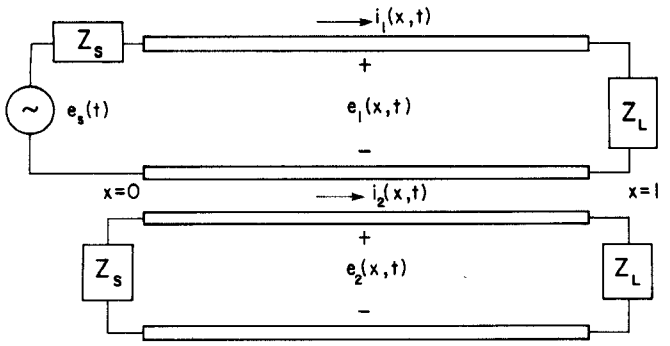


Fig. 1. Circuit diagram for coupled transmission lines.

tions:

$$\frac{\partial e_1}{\partial x} + L_1\frac{\partial i_1}{\partial t} + L_m\frac{\partial i_2}{\partial t} = 0 \tag{1a}$$

$$\frac{\partial e_2}{\partial x} + L_m\frac{\partial i_1}{\partial t} + L_2\frac{\partial i_2}{\partial t} = 0 \tag{1b}$$

$$\frac{\partial i_1}{\partial x} + C_1\frac{\partial e_1}{\partial t} - C_m\frac{\partial e_2}{\partial t} = 0 \tag{1c}$$

$$\frac{\partial i_2}{\partial x} - C_m\frac{\partial e_1}{\partial t} + C_2\frac{\partial e_2}{\partial t} = 0 \tag{1d}$$

where $L_1, L_2, C_1, C_2, L_m, C_m$ are all functions of position $x$. From the transmission-line theory, we know that these parameters are related to the impedance parameters $L_{10}, L_{20}, C_{10}, C_{20}$ [19] by

$$\left.\begin{aligned} L_i &= L_{i0} - L_m \\ C_i &= C_{i0} + C_m \end{aligned}\right\} \quad \text{for } i=1,2. \tag{2}$$

### A. Coupled-Mode Analysis

The first step is to decouple the four equations into two separate pairs. We use the following transformations [19]:

$$a_{i\pm} = \frac{1}{\sqrt{2Z_i}}(e_i \pm Z_i i_i) \qquad \text{for } i=1,2 \tag{3}$$

where

$$Z_i(x) = \sqrt{L_i(x)/C_i(x)}, \qquad i=1,2$$

stand for self characteristic impedances for individual lines. We assume that both lines have equal phase velocity

$$\frac{1}{\sqrt{L_1C_1}} = \frac{1}{\sqrt{L_2C_2}} = v \tag{4}$$

and that the propagating modes on the lines are quasi-TEM. The inductive coupling coefficient $k_L$ and the capacitive coupling coefficient $k_C$ are equal, and we can discard the subscripts $L, C$ and write

$$k = \frac{L_m}{\sqrt{L_1L_2}} = \frac{C_m}{\sqrt{C_1C_2}}. \tag{5}$$

For conciseness, we express the transformed equations in matrix form

$$\frac{\partial A}{\partial x} + \begin{pmatrix} \Omega & 0 \\ 0 & -\Omega \end{pmatrix}\frac{\partial A}{\partial t} + \begin{pmatrix} 0 & P \\ P & 0 \end{pmatrix}A = 0 \tag{6}$$

where

$$A = (a_{1+} \quad a_{2-} \quad a_{1-} \quad a_{2+})^t$$

$$\Omega = \frac{1}{v}\begin{pmatrix} 1 & -k \\ k & -1 \end{pmatrix}$$

and

$$P = \begin{pmatrix} p_1 & 0 \\ 0 & p_2 \end{pmatrix}$$

in which $p_i = d[\ln\sqrt{Z_i(x)}\,]/dx$. The transformation given by (3) is known as the codirectional–contradirectional decomposition for coupled-mode equations.

### B. Solution by Method of Characteristics

The solution to (6) is complicated by the presence of $p_1, p_2$. In fact, there is no general analytical technique unless $Z_1$ and $Z_2$ are independent of position $x$, which was the case discussed in [19]. In this paper, however, we shall be able to treat more general cases for which $Z_i(x)$ and $k(x)$ are slowly-varying functions of $x$ using a combination of the method of characteristics and perturbational series.

Mathematically (6) is a hyperbolic system of partial differential equations and the method of characteristics is a standard way of solving this kind of problem. To apply the method of characteristics, there can be, firstly, only one dependent variable in derivative terms of any individual equation, and, secondly, for each equation, we then form a family of curves called *characteristics* on which the equation involved becomes an ordinary differential equation [20].

To satisfy the first requirement, we introduce the transformation

$$Y = \begin{pmatrix} T & 0 \\ 0 & T \end{pmatrix}A \tag{7}$$

where $Y = (F \; B \; b \; f)^t$ and $T$ must diagonalize $\Omega$. When expressed in terms of $Y$, the matrix equation becomes

$$\frac{\partial Y}{\partial x} + \begin{pmatrix} \lambda_+ & 0 & 0 & 0 \\ 0 & \lambda_- & 0 & 0 \\ 0 & 0 & \lambda_- & 0 \\ 0 & 0 & 0 & \lambda_+ \end{pmatrix}\frac{\partial Y}{\partial t} = \tilde{P}Y. \tag{8}$$

There are two families of characteristics for (8), each associated with two dependent variables among the four.

1) For $F$ and $f$, the parametric equations of the characteristics family $\Gamma_1$ are

$$\frac{dx}{ds_1} = 1 \qquad \frac{dt}{ds_1} = \lambda_+ \tag{9}$$

or, after canceling $s_1$

$$t - \int \lambda_+ \, dx = \text{const.} \tag{10}$$

And on any characteristic curve, we have

$$\frac{dF}{ds_1} = \tilde{p}_{11}F + \tilde{p}_{12}B + \tilde{p}_{13}b + \tilde{p}_{14}f \tag{11a}$$

$$\frac{df}{ds_1} = \tilde{p}_{41}F + \tilde{p}_{42}B + \tilde{p}_{43}b + \tilde{p}_{44}f. \tag{11b}$$

2) For $B$ and $b$, the characteristics family $\Gamma_2$ is specified by

$$\frac{dx}{ds_2}=1 \quad \frac{dt}{ds_2}=\lambda_- \tag{12}$$

or

$$t-\int\lambda_- dx=\text{const.} \tag{13}$$

On any characteristic curve, we have

$$\frac{dB}{ds_2}=\tilde{p}_{21}F+\tilde{p}_{22}B+\tilde{p}_{23}b+\tilde{p}_{24}f \tag{14a}$$

$$\frac{db}{ds_2}=\tilde{p}_{31}F+\tilde{p}_{32}B+\tilde{p}_{33}b+\tilde{p}_{34}f. \tag{14b}$$

In theory, we can numerically integrate (11) and (14) on the characteristics to solve the problem. Indeed, this is the scheme adopted in some previous work for a single transmission line, e.g., [18]. However, these ordinary differential equations are coupled; thus, the numerical integrations become more and more difficult as the number of lines increases. The way to get around this is to resort to perturbational series. We need to elaborate on the transformation (7). Besides diagonalizing $\Omega$, we further require the diagonal terms of $\tilde{P}$ to be zero. All such $T$ can be written explicitly as

$$T=c(1-k^2)^{-1/4}\begin{pmatrix}\sqrt{1+k}+\sqrt{1-k} & \sqrt{1-k}-\sqrt{1+k}\\ \sqrt{1-k}-\sqrt{1+k} & \sqrt{1+k}+\sqrt{1-k}\end{pmatrix} \tag{15}$$

where $c$ is an arbitrary constant. For convenience, we choose $c=1$. The related quantities are given as follows:

$$\lambda_-=-\lambda_+=\frac{1}{v}\sqrt{1-k^2} \tag{16}$$

and

$$\tilde{P}=\begin{pmatrix}0 & \frac{-k'}{2(1-k^2)} & p_{11} & p_{12}\\ \frac{-k'}{2(1-k^2)} & 0 & p_{21} & p_{22}\\ p_{11} & p_{12} & 0 & \frac{-k'}{2(1-k^2)}\\ p_{21} & p_{22} & \frac{-k'}{2(1-k^2)} & 0\end{pmatrix} \tag{17}$$

where $p_{11}$, $p_{12}$, $p_{21}$, $p_{22}$ are the same order as $p_1$, $p_2$. With our assumptions on $k(x)$ and $p_i(x)$, we expect $\tilde{P}Y$ in (8) to be small as compared with the terms on the left-hand side. Therefore, we formally construct a perturbational series representation of the solution

$$Y=\begin{pmatrix}F\\B\\b\\f\end{pmatrix}=\begin{pmatrix}F^{(0)}\\B^{(0)}\\b^{(0)}\\f^{(0)}\end{pmatrix}+\begin{pmatrix}F^{(1)}\\B^{(1)}\\b^{(1)}\\f^{(1)}\end{pmatrix}+\cdots. \tag{18}$$

The following iterative equations are obtained:

$$\frac{dF^{(n+1)}}{ds_1}=-\frac{k'}{2(1-k^2)}B^{(n)}+p_{11}b^{(n)}+p_{12}f^{(n)} \tag{19a}$$

$$\frac{dB^{(n+1)}}{ds_2}=-\frac{k'}{2(1-k^2)}F^{(n)}+p_{21}b^{(n)}+p_{22}f^{(n)} \tag{19b}$$

$$\frac{db^{(n+1)}}{ds_2}=-\frac{k'}{2(1-k^2)}f^{(n)}+p_{11}F^{(n)}+p_{12}B^{(n)} \tag{19c}$$

$$\frac{df^{(n+1)}}{ds_1}=-\frac{k'}{2(1-k^2)}b^{(n)}+p_{21}F^{(n)}+p_{22}B^{(n)}. \tag{19d}$$

The problem is simplified considerably because of the following.

1) The zeroth-order equations

$$\frac{dF^{(0)}}{ds_1}=\frac{dB^{(0)}}{ds_2}=\frac{db^{(0)}}{ds_2}=\frac{df^{(0)}}{ds_1}=0$$

have closed-form solutions

$$F^{(0)}=F_0\left(t-\int\lambda_+ dx\right), \qquad f^{(0)}=f_0\left(t-\int\lambda_+ dx\right) \tag{20a}$$

$$B^{(0)}=B_0\left(t+\int\lambda_+ dx\right), \qquad b^{(0)}=b_0\left(t+\int\lambda_+ dx\right). \tag{20b}$$

2) All higher order terms are generated from single integration over the previous order terms, hence there are no unknowns on the right-hand sides of (19a)–(19d) as we carry out the iteration steps. The coupled ordinary differential equations (11) and (14) are now reduced to a problem involving a simple indefinite integral.

Physically, every characteristic curve stands for a constant phase front, and every expression in (20) represents a traveling wave of constant amplitude. $F^{(0)}$ and $f^{(0)}$ propagate along the $(+x)$-direction, while $B^{(0)}$ and $b^{(0)}$ propagate along the $(-x)$-direction, and with the same speed. All higher order terms have similar properties as the corresponding zeroth-order terms, except that the amplitudes no longer remain constant as the waves propagate because the right-hand sides of (19a)–(19d) are not zero.

In the following section, we shall demonstrate the power of this perturbational approach and its physical significance by applying it to a wide class of problems.

## III. Perturbational Analysis of a Pair of Identical Lines

As an example, consider the case when the two lines have identical parameters. We further assume that $L_{10}=L_{20}=L_0=\text{const.}$ and $C_{10}=C_{20}=C_0=\text{const.}$ Thus, the

phase velocity $c_0$ and characteristic impedance $Z_0$, defined by

$$c_0 = 1/\sqrt{L_0 C_0}$$

and

$$Z_0 = \sqrt{L_0/C_0}$$

respectively, will also be independent of position $x$. From (2) and (5), we can then express the line parameters in terms of $L_0$, $C_0$, and $k(x)$

$$L_1(x) = L_2(x) = L_0/(1+k(x))$$
$$C_1(x) = C_2(x) = C_0/(1-k(x)).$$

Thus

$$Z_1(x) = Z_2(x) = \sqrt{\frac{L_1}{C_1}} = Z_0\sqrt{\frac{1-k}{1+k}}$$

and

$$p_1 = p_2 = \frac{1}{4}\frac{d}{dx}\ln\frac{1-k}{1+k} = -\frac{k'}{2(1-k^2)}. \tag{21}$$

We also find that

$$\lambda_+ = \sqrt{1-k^2}\sqrt{L_1C_1} = \sqrt{L_0C_0} = 1/c_0. \tag{22}$$

The characteristics curves are straight lines in $x-t$ space, thus eliminating the need to numerically evaluate $\int \lambda_+ \, dx$.

With $p_1$ and $p_2$ known, we then calculate $p_{11}$, $p_{12}$, $p_{21}$, $p_{22}$ and obtain the following explicit form for the iterative equations:

$$\frac{dF^{(n+1)}}{ds_1} = -\frac{k'}{2(1-k^2)}B^{(n)} + \frac{k'}{2(1-k^2)}b^{(n)} \tag{23a}$$

$$\frac{dB^{(n+1)}}{ds_2} = -\frac{k'}{2(1-k^2)}F^{(n)} + \frac{k'}{2(1-k^2)}f^{(n)} \tag{23b}$$

$$\frac{db^{(n+1)}}{ds_2} = -\frac{k'}{2(1-k^2)}f^{(n)} + \frac{k'}{2(1-k^2)}F^{(n)} \tag{23c}$$

$$\frac{df^{(n+1)}}{ds_1} = -\frac{k'}{2(1-k^2)}b^{(n)} + \frac{k'}{2(1-k^2)}B^{(n)}. \tag{23d}$$

Here (23a) and (23d) are valid only along the curves of the characteristics family $\Gamma_1$, specified by $t - x/c_0 =$ constant, whereas (23b) and (23c) are valid only along the curves of the characteristics family $\Gamma_2$ specified by $t + x/c_0 =$ constant.

Suppose the excitation voltage is $e_s(t) = u(t)$ and both ends of the two lines are matched, i.e., $Z_L = Z(l)$, $Z_s = Z(0)$, the initial states will be zero for any dependent variable and the boundary conditions for $a_{1+}$, $a_{1-}$, $a_{2+}$, $a_{2-}$ are

$$a_{1+}(0,t) = u(t)/\sqrt{2Z_s} \tag{24a}$$

$$a_{2-}(l,t) = 0 \tag{24b}$$

$$a_{1-}(l,t) = 0 \tag{24c}$$

$$a_{2+}(0,t) = 0. \tag{24d}$$

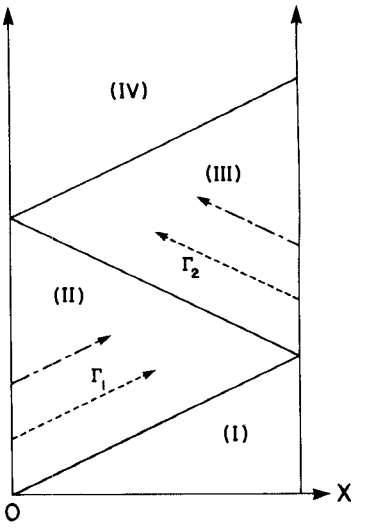


Fig. 2. Two families of characteristics.

In view of transformation (15), the reflection coefficients at the boundaries are determined by these boundary conditions:

$$F^{(0)}(0,t) = \frac{4(1-k^2(0))^{1/4}}{\sqrt{2Z_s}\sqrt{1-k(0)}+\sqrt{1+k(0)}}u(t) + R(0)B^{(0)}(0,t) \tag{25a}$$

$$F^{(n)}(0,t) = R(0)\cdot B^{(n)}(0,t) \quad \text{for } n \neq 0 \tag{25b}$$

$$B^{(n)}(l,t) = R(l)\cdot F^{(n)}(l,t) \tag{25c}$$

$$f^{(n)}(0,t) = R(0)\cdot b^{(n)}(0,t) \tag{25d}$$

$$b^{(n)}(l,t) = R(l)\cdot f^{(n)}(l,t) \tag{25e}$$

where

$$R(p) = \frac{\sqrt{1-k(p)}-\sqrt{1+k(p)}}{\sqrt{1-k(p)}+\sqrt{1+k(p)}}.$$

### *A. Zeroth-Order Solutions*

The solutions to the zeroth-order equations can be represented as infinite series, which arise from reflections at both ends. The propagation diagram in $x-t$ space (Fig. 2) would be of use to our derivation. Judging from the homogeneous boundary conditions (25d) and (25e), we conclude that $f^{(0)} \equiv b^{(0)} \equiv 0$. Because the procedures for solving $F^{(0)}$ and $B^{(0)}$ are analogous to those for uniformly coupled lines, we simply give their analytical expressions in the final form.

*Region* (I): $t - x/c_0 < 0$

$$F^{(0)} = B^{(0)} = 0. \tag{26}$$

This is consistent with causality.

In the following expressions, $T = l/c_0$.

*Region* (II): $x/c_0 \leqslant t < 2T - x/c_0$

$$F^{(0)}(x,t) = \frac{4(1-k^2(0))^{1/4}u(t-x/c_0)}{\sqrt{2Z_s}\left(\sqrt{1+k(0)}+\sqrt{1-k(0)}\right)}. \tag{27a}$$

$$B^{(0)}(x,t) = 0 \tag{27b}$$

Either there is no backward mode due to reflection at $x = l$ or it has yet to reach the observer.

*Region* (III): $2T - x/c_0 \leqslant t < 2T + x/c_0$

$$F^{(0)}(x,t) = \frac{4(1-k^2(0))^{1/4} u(t - x/c_0)}{\sqrt{2Z_s}\left(\sqrt{1+k(0)} + \sqrt{1-k(0)}\right)} \tag{28a}$$

$$B^{(0)}(x,t) = R(l) \cdot \frac{4(1-k^2(0))^{1/4} u(t + x/c_0 - 2T)}{\sqrt{2Z_s}\left(\sqrt{1+k(0)} + \sqrt{1-k(0)}\right)}. \tag{28b}$$

The backward mode is received, but the second reflection at $x = 0$ has not yet been observed.

*Region* (IV): $2T + x/c_0 \leqslant t < 4T - x/c_0$

$$F^{(0)}(x,t) = \frac{4(1-k^2(0))^{1/4}}{\sqrt{2Z_s}\left(\sqrt{1+k(0)} + \sqrt{1-k(0)}\right)} \cdot \left[u(t - x/c_0) + R(l) \cdot R(0) \cdot u(t - x/c_0 - 2T)\right] \tag{29a}$$

$$B^{(0)}(x,t) = R(l) \cdot \frac{4(1-k^2(0))^{1/4}}{\sqrt{2Z_s}\left(\sqrt{1+k(0)} + \sqrt{1-k(0)}\right)} \cdot u(t + x/c_0 - 2T). \tag{29b}$$

Now we have a double reflection term in the forward mode.

Continuing the analysis, we can find the series representations for both $F^{(0)}$ and $B^{(0)}$; they are

$$F^{(0)}(x,t) = \frac{4(1-k^2(0))^{1/4}}{\sqrt{2Z_s}\left(\sqrt{1+k(0)} + \sqrt{1-k(0)}\right)} \cdot \sum_{n=0}^{\infty} \left[R(0) \cdot R(l)\right]^n u(t - x/c_0 - 2nT) \tag{30a}$$

$$B^{(0)}(x,t) = \frac{4(1-k^2(0))^{1/4}}{\sqrt{2Z_s}\left(\sqrt{1+k(0)} + \sqrt{1-k(0)}\right)} \cdot R(l) \sum_{n=0}^{\infty} \left[R(0) \cdot R(l)\right]^n u(t + x/c_0 - 2(n+1)T). \tag{30b}$$

Applying the inverse transformation of (15), we get the expressions for $a_{1+}$ and $a_{2-}$

$$a_{1+} = \frac{(1-k^2(0))^{1/4}}{\sqrt{2Z_s}(1-k^2(x))^{1/4}} \left\{ \frac{\sqrt{1+k(x)} + \sqrt{1-k(x)}}{\sqrt{1+k(0)} + \sqrt{1-k(0)}} \sum_{n=0}^{\infty} \left[R(0) \cdot R(l)\right]^n u(t - x/c_0 - 2nT) + \frac{\left(\sqrt{1+k(x)} - \sqrt{1-k(x)}\right)}{\left(\sqrt{1-k(0)} + \sqrt{1+k(0)}\right)} \cdot R(l) \sum_{n=0}^{\infty} \left[R(0) \cdot R(l)\right]^n u(t + x/c_0 - 2(n+1)T) \right\} \tag{31a}$$

$$a_{2-} = \frac{(1-k^2(0))^{1/4}}{\sqrt{2Z_s}(1-k^2(x))^{1/4}} \left\{ \frac{\sqrt{1+k(x)} - \sqrt{1-k(x)}}{\sqrt{1+k(0)} + \sqrt{1-k(0)}} \sum_{n=0}^{\infty} \left[R(0) \cdot R(l)\right]^n u(t - x/c_0 - 2nT) + \frac{\left(\sqrt{1-k(x)} + \sqrt{1+k(x)}\right)}{\left(\sqrt{1-k(0)} + \sqrt{1+k(0)}\right)} \cdot R(l) \sum_{n=0}^{\infty} \left[R(0) \cdot R(l)\right]^n u(t + x/c_0 - 2(n+1)T) \right\}. \tag{31b}$$

The zeroth-order expressions are exactly what one would get by solving this problem with WKB approximations in the frequency domain and transforming back to the time domain (see Appendix). We notice that both forward and backward propagating modes are only initiated from the boundaries. Although there are amplitude variations with distance, we see no reflection terms generated between both boundaries, which should arise in view of the nonuniform coupling. Apparently, more terms need to be included to account for this behavior.

### B. First-Order Solutions

A close look at (23a)–(23d) reveals that the $(n+1)$th-order forward modes depend only on the $n$th-order backward modes explicitly, and a similar relation exists between the $(n+1)$th backward modes and the $n$th forward modes. This fact enables us to interpret the higher order terms to be the reflections due to nonuniform coupling along the lines. Note that if we had not chosen the transformation (15), the physical meaning of the iterative equations would not be so clear.

The integration of (23) becomes even easier for the first-order terms if we make use of (9) and (12), which guarantee that we can substitute $d/ds_1$ and $d/ds_2$ by $d/dx$ on corresponding characteristics. Together with $f^{(0)} = b^{(0)} = 0$, we obtain

$$\frac{dF^{(1)}}{dx} = -\frac{k'}{2(1-k^2)} B^{(0)} \tag{32a}$$

$$\frac{dB^{(1)}}{dx} = -\frac{k'}{2(1-k^2)} F^{(0)} \tag{32b}$$

$$\frac{db^{(1)}}{dx} = \frac{k'}{2(1-k^2)} F^{(0)} \tag{32c}$$

$$\frac{df^{(1)}}{dx} = \frac{k'}{2(1-k^2)} B^{(0)}. \tag{32d}$$

Under unit step excitation, $F^{(0)}$ and $B^{(0)}$ being constant within each region as shown in Fig. 2, (32a)–(32d) will have closed-form solutions.

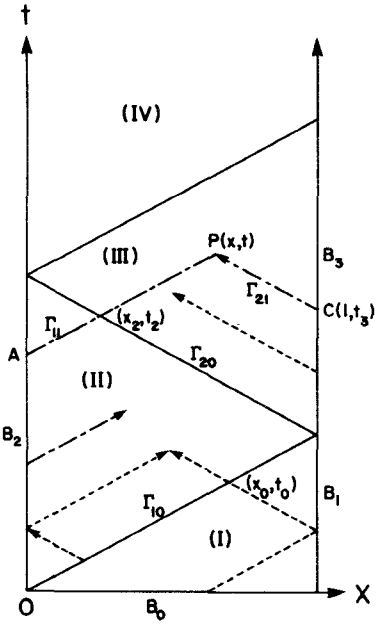


Fig. 3. Integration paths on $x-t$ space.

With the help of the auxiliary diagram (Fig. 3), we now construct the first-order solutions as follows.

*Region* (I): $t < x/c_0$

Integration starts from $B_0$ and $B_1$ along the directions specified. With zero initial condition and null zeroth-order terms, we conclude that first-order terms disappear. In fact, with the same reasoning, causality automatically holds for higher order terms.

*Region* (II): $x/c_0 \leqslant t < 2T - x/c_0$

From the previous analysis, $B(0) = 0$ and $F(0) = F_0$, a constant. Integration starts from $(x_0, t_0)$ on $\Gamma_{10}$, and along $\Gamma_2$. We find that

$$B^{(1)}(x,t) = \frac{F_0}{4} \ln \frac{(1-k(x))(1+k(x_0))}{(1+k(x))(1-k(x_0))} \tag{33a}$$

$$b^{(1)}(x,t) = \frac{F_0}{4} \ln \frac{(1+k(x))(1-k(x_0))}{(1-k(x))(1+k(x_0))} \tag{33b}$$

where $x_0 = (x + c_0 t)/2$.

Substituting $x$ by 0, we find the boundary values on $B_2$ for future use

$$B^{(1)}(0,t) = \frac{F_0}{4} \ln \frac{(1-k(0))(1+k(c_0 t/2))}{(1+k(0))(1-k(c_0 t/2))} \tag{34a}$$

$$b^{(1)}(0,t) = \frac{F_0}{4} \ln \frac{(1+k(0))(1-k(c_0 t/2))}{(1-k(0))(1+k(c_0 t/2))} \tag{34b}$$

$$F^{(1)}(0,t) = R(0) \cdot \frac{F_0}{4} \ln \frac{(1-k(0))(1+k(c_0 t/2))}{(1+k(0))(1-k(c_0 t/2))} \tag{34c}$$

$$f^{(1)}(0,t) = R(0) \cdot \frac{F_0}{4} \ln \frac{(1+k(0))(1-k(c_0 t/2))}{(1-k(0))(1+k(c_0 t/2))}. \tag{34d}$$

Because $B^{(0)} = 0$, $F^{(1)}$ and $f^{(1)}$ are constant along any characteristics $\Gamma_1$. Denoting $F^{(1)}(0,t)$, $f^{(1)}(0,t)$ by $F_{11}(t)$, $f_{11}(t)$, we can express $F^{(1)}$ and $f^{(1)}$ as

$$F^{(1)}(x,t) = F_{11}(t - x/c_0) \tag{35a}$$

$$f^{(1)}(x,t) = f_{11}(t - x/c_0). \tag{35b}$$

*Region* (III): $2T - x/c_0 \leqslant t < 2T + x/c_0$

The zeroth-order terms are

$$F^{(0)} = F_0$$

$$B^{(0)} = R(l) F_0.$$

Starting from $\Gamma_{20}$, we integrate $F^{(1)}$, $f^{(1)}$ along $\Gamma_1$ and find that

$$F^{(1)}(x,t) = \frac{R(l)F_0}{4} \ln \frac{(1-k(x))(1+k(x_2))}{(1+k(x))(1-k(x_2))} + F_{11}\left(t_2 - \frac{x_2}{c_0}\right) \tag{36a}$$

$$f^{(1)}(x,t) = \frac{R(l)F_0}{4} \ln \frac{(1+k(x))(1-k(x_2))}{(1-k(x))(1+k(x_2))} + f_{11}\left(t_2 - \frac{x_2}{c_0}\right) \tag{36b}$$

where

$$x_2 = c_0 T + (x - c_0 t)/2$$

$$t_2 = T + (t - x/c_0)/2.$$

In this manner, the boundary values of $F^{(1)}, f^{(1)}$ on $B_3$ can be obtained. Denoting them by $F_{12}(t), f_{12}(t)$, we then integrate on $\Gamma_2$ to find $B^{(1)}, b^{(1)}$ as follows:

$$B^{(1)}(x,t) = \frac{F_0}{4} \ln \frac{(1-k(x))(1+k(l))}{(1+k(x))(1-k(l))} + R(l) F_{12}\left(t + \frac{x}{c_0} - \frac{l}{c_0}\right) \tag{37a}$$

$$b^{(1)}(x,t) = \frac{F_0}{4} \ln \frac{(1+k(x))(1-k(l))}{(1-k(x))(1+k(l))} + R(l) f_{12}\left(t + \frac{x}{c_0} - \frac{l}{c_0}\right). \tag{37b}$$

For all the other regions, similar procedures apply. In general, there are always two characteristics passing through any interior point $P(x,t)$. We extend $\Gamma_1$ to the left boundary ($x = 0$), $\Gamma_2$ to the right boundary ($x = l$). The boundary values for two modes can always be found with the same scheme and the remaining two are obtained from reflection conditions. As soon as the boundary values are found, we integrate along the curve to get the value at $P$.

With this scheme, we do not have to find all the boundary values nor all the lower order terms in the whole $x-t$ domain. For instance, in Fig. 3, we only need boundary values up to $A$ and $C$ and lower order terms up to $\Gamma_{11}$ and $\Gamma_{21}$ in order to find the value at $P$.

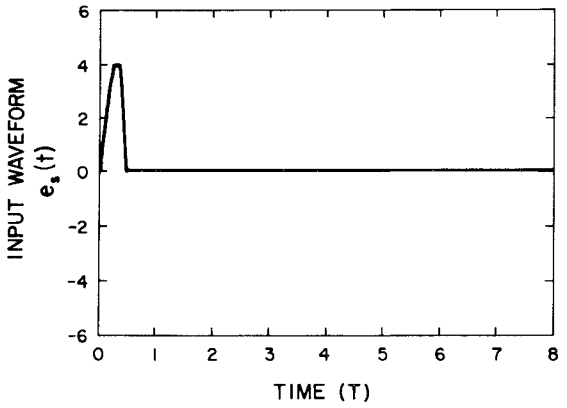


Fig. 4. Input waveform.

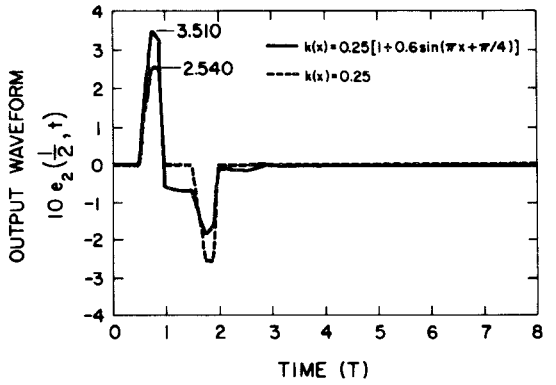


Fig. 5. Responses on line 2 for $k(x) = 0.25[1 + 0.6\sin(\pi x + \pi/4)]$ (———) and $k(x) = 0.25$ (---).

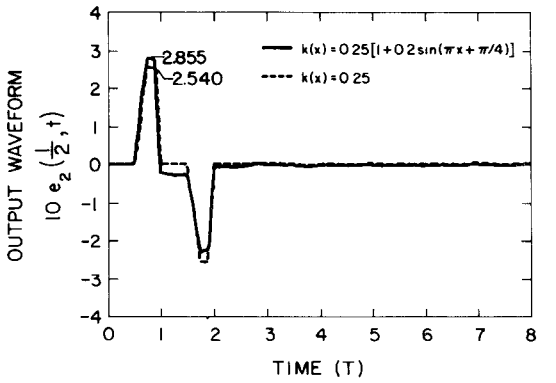


Fig. 6. Responses on line 2 for $k(x) = 0.25[1 + 0.2\sin(\pi x + \pi/4)]$ (———) and $k(x) = 0.25$ (---).

## IV. Results

While the analysis in previous section assumes unit step excitation, the response due to general inputs can be easily evaluated through convolution.

In this section, we present some numerical results to verify our perturbational analysis and to examine the overall effect of nonuniform coupling. For convenience, both the time scale and the position scale are normalized such that $l = 1$ and $T = 1$. The input waveform in Fig. 4 is used as the excitation voltage on line 1 throughout our calculation. It has a rise time of 0.125 $T$, and a fall-off time of 0.0625 $T$. The impedance at the start of each line is $Z_s = 50$

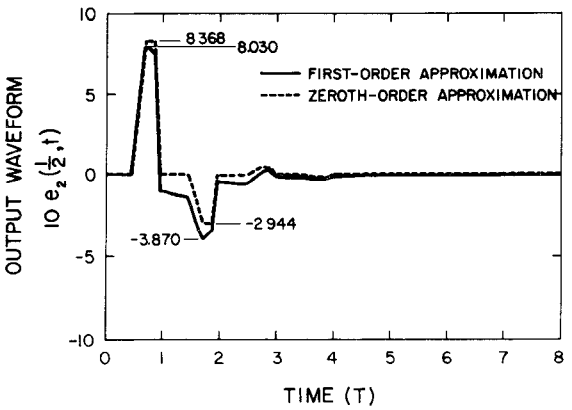


Fig. 7. Comparison of zeroth-order approximation with first-order approximation for $k(x) = 0.5[1 + 0.6\sin(\pi x + \pi/4)]$.

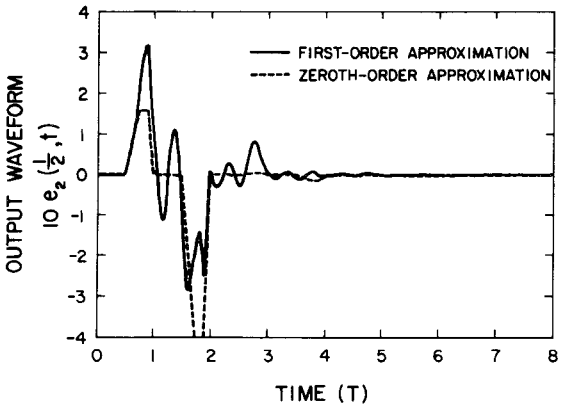


Fig. 8. Comparison of zeroth-order approximation with first-order approximation for $k(x) = 0.5[1 + 0.6\sin(10\pi x + \pi/4)]$.

Ω. The output waveforms shown in all figures are taken at the midpoints of the lines; and the magnitudes are ten times the actual size.

In Figs. 5 and 6, we compare the output on line 2 for both uniformly coupled and nonuniformly coupled cases. The coupling coefficients are $k \equiv 0.25$ for the dashed lines in Figs. 5 and 6, $k(x) = 0.25[1 + 0.6\sin(\pi x + \pi/4)]$ for the solid line in Fig. 5, and $k(x) = 0.25[1 + 0.2\sin(\pi x + \pi/4)]$ for the solid line in Fig. 6. The peak values of the waveforms associated with nonuniform coupling coefficients indicate that the solid line (nonuniform coupling) is closer to the dashed line (uniform coupling) in Fig. 6 than in Fig. 5, as is expected since the coupling coefficient for the former case is closer to that for the uniform case. This ensures the stability of the solutions.

We also need to confirm our construction of perturbational series. The two waveforms in Fig. 7 are, respectively, the zeroth-order approximation (dashed line) and the first-order approximation (solid line) to the response on line 2 for $k(x) = 0.5[1 + 0.6\sin(\pi x + \pi/4)]$. Note that though $k$ can be as large as 0.8, the two approximations are quite close, judging from the peak values. Therefore, we are sure that the first-order solutions indeed can be treated as perturbational terms.

Of course, when our assumption of slowly varying $k(x)$ does not hold, the first-order solution may not be suffi-

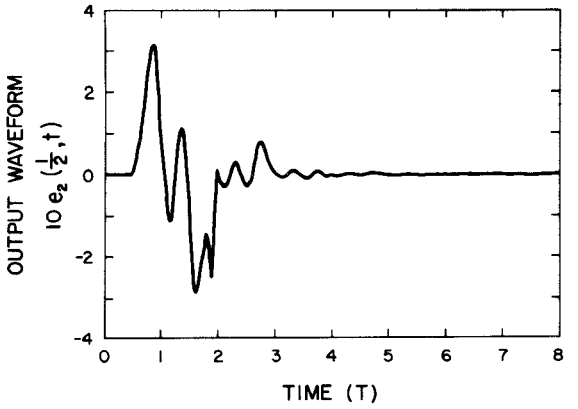


Fig. 9. Response on line 2 for $k(x) = 0.5[1 + 0.6\sin(10\pi x + \pi/4)]$.

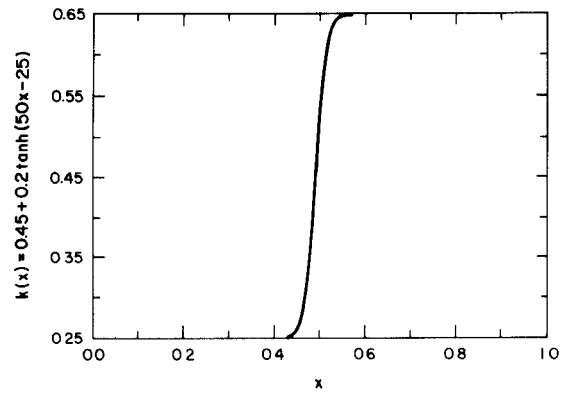


Fig. 10. $k(x)$ versus position for $k(x) = 0.45 + 0.2\tanh(50x - 25)$.

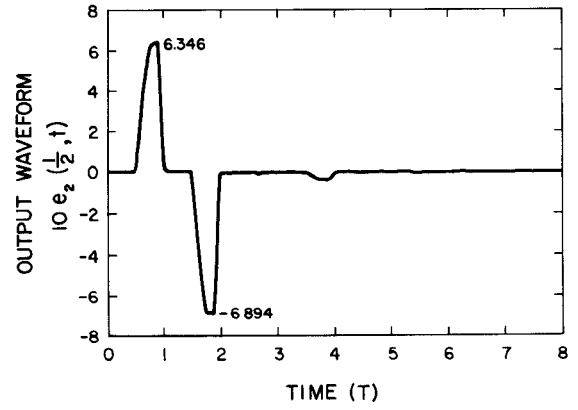


Fig. 11. Response on line 2 for $k(x) = 0.45 + 0.2\tanh(50x - 25)$.

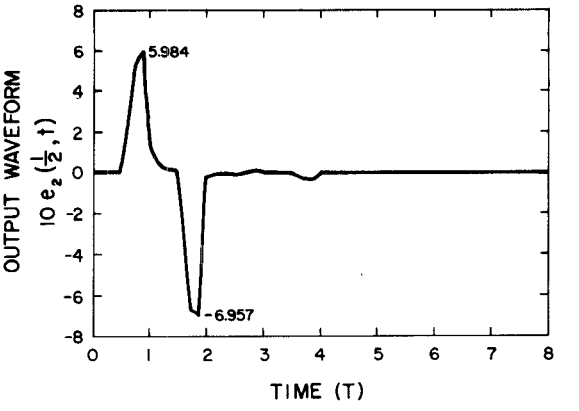


Fig. 12. Response on line 2 for $k(x) = 0.45 + 0.2\tanh(10x - 5)$.

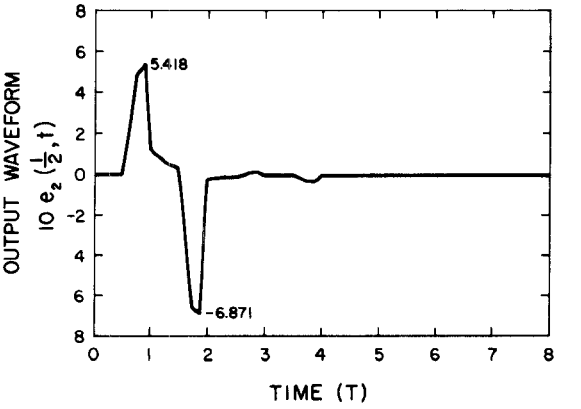


Fig. 13. Response on line 2 for $k(x) = 0.45 + 0.2\tanh(5.0x - 2.5)$.

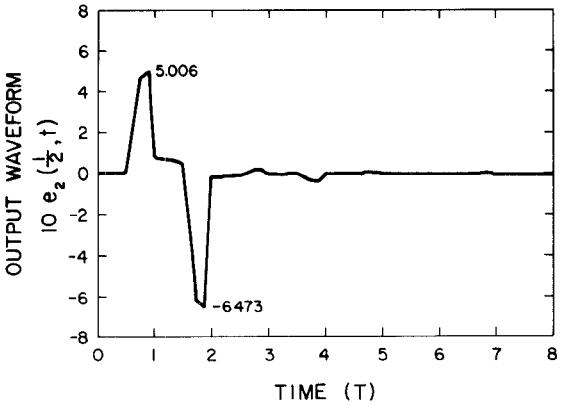


Fig. 14. Response on line 2 for $k(x) = 0.45 + 0.2\tanh(2.5x - 1.25)$.

cient. For example, in Fig. 8, $k(x) = 0.25[1 + 0.6\sin(10\pi x + \pi/4)]$, the two approximations differ significantly. But by counting the number of peaks and troughs in one single trip from end to end, the first-order approximation does give some information about the variation of $k(x)$.

We note that $k(x)$ may also be slowly-varying yet change drastically in a small region. In that case, the first-order approximation still yields accurate results. This is illustrated in Fig. 9. Shown in Fig. 10 is the plot of $k(x)$ versus position $x$ with $k(x) = 0.45 + 0.2\tanh(50x - 25)$. A heuristic approximation to this system is two segments of uniformly coupled lines with distinct $k(x)$'s joined together at the midpoint. The response on line 2 is plotted in Fig. 11. We discover that it is similar to what would be observed at the junction of two segments described above.

With $k(x)$ of the form $a + b\tanh(2cx - c)$, we can investigate the effects of different lengths of the transition region between two distinct segments. In Figs. 12–14, $a, b$ are the same as in Fig. 11, and $c = 5.0, 2.5, 1.25$ for Figs. 12–14, respectively. It is found that as the transition becomes more gradual, or $c$ decreases, the peak values of the response on line 2 decrease, but spread over longer period.

The responses on line 1 are less sensitive to the transition lengths of $k(x)$. Figs. 15 and 16 show the responses for $c = 1.25$ and $c = 2.5$, respectively. Of course, as $c$ increases,

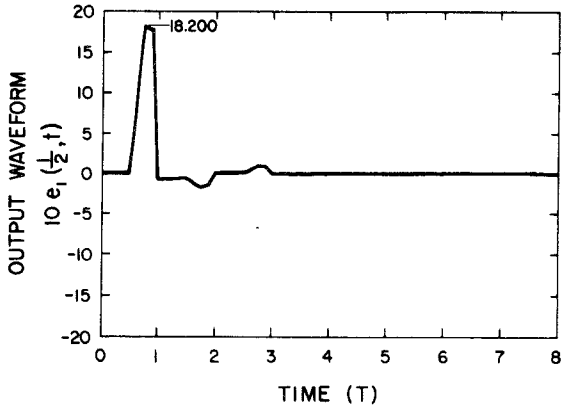


Fig. 15. Response on line 1 for $k(x) = 0.45 + 0.2\tanh(2.5x - 1.25)$.

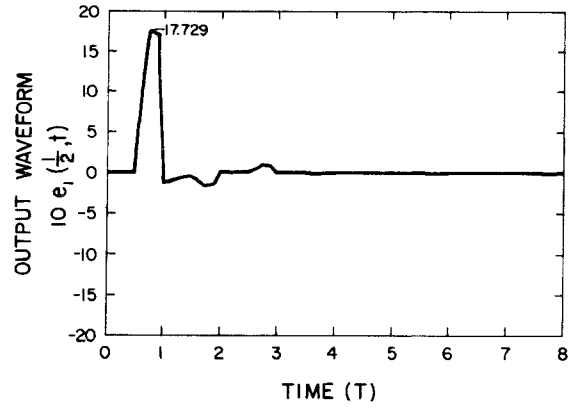


Fig. 16. Response on line 1 for $k(x) = 0.45 + 0.2\tanh(5.0x - 2.5)$.

the peak values attenuate because more energy is transferred to line 2.

In all the figures, the resolution is 60 points/$T$ and we consider values up to $8T$. The computation time ranges from 1 to 2.5 on a VAX 11/750, depending mostly on the number of output data sets required and the time spent in evaluating $k(x)$, since few algebraic calculations are involved. The convolutions are done within 3 s. There would be a considerable reduction in time if $k(x)$ are obtained by table look-up. Because the graphical results show that calculations up to $4T$ will be enough for most applications, the computation time can be cut even further.

## V. Conclusions

A general time-domain formulation for two nonuniformly coupled dispersionless transmission lines has been developed with the aid of the perturbational series. Causality and the reflections along the lines are automatically included in the solution. For the simplest case with two identical lines having arbitrary coupling coefficient $k(x)$, we have shown that closed-form solutions can be obtained up to first order in $k$. The higher order terms are generated iteratively, though the results indicate that we seldom need to go beyond the first-order approximation. The implementation of the algorithm simply involves stepping in the $x-t$ domain. Only the data involving past-time are needed for integration along the characteristics. The integrands contain only the next lower order terms. Compared to frequency-domain techniques, it also provides more physical insight. As indicated in Section III, the basic approximation derived from the WKB method contains only the wavefront and the amplitude information associated with the two modes bouncing back and forth between two ends. Higher order WKB analyses or perturbational series representation [22] in the frequency domain are considerably complicated, let alone needing a final Fourier inversion, and the results are hard to explain physically. On the other hand, the direct time-domain perturbational approach is much easier to handle, as given by the previous sections. it can be extended to other cases, such as when the loads are not matched. Here $f^{(0)}$ and $b^{(0)}$ will not be zero, and all we have to do is to include their contributions in the integration, which will still be in closed form for a unit step input. If the loads are not purely resistive, or time-varying, or even nonlinear, the techniques described by Mohammadian and Tai [11], [13], [21] can be accommodated to yield the appropriate reflection conditions. In general, as long as there is no dispersion, this method is most efficient and accurate for transient analysis purpose. As for prospective future works, we feel that it is possible to treat the problems in which the phase velocities of the two lines are not equal by modifying the transformation matrix $T$, although closed-form solutions may be hard to come by. For the structures involving multiple coupled lines, the concept of coupling coefficients is not that useful. But one shall still find it easier to look for perturbational solutions by numerical integration than to solve the original coupled partial differential equations.

## Appendix
## Asymptotic Solution by Transform Method

Assuming $e^{j\omega t}$ dependence, the frequency-domain counterpart of (6) is

$$\frac{d\hat{A}}{dx} + j\beta\begin{pmatrix}\Omega & 0\\ 0 & -\Omega\end{pmatrix}\hat{A} + \begin{pmatrix}0 & P\\ P & 0\end{pmatrix}\hat{A} = 0 \qquad \text{(A1)}$$

where $\hat{A}$ is the Fourier transform of $A$, $\beta = \omega/v$, and $p_1 = p_2 = -k'/(1-k^2)$ as given by (21).

As far as the transient behavior is concerned, we can apply high-frequency approximation techniques. For the present case, the WKB physical optics approximation is a natural choice.

We would neglect the third terms in (A1), since $\beta > \beta k \gg k'/2(1-k^2)$. Again, we obtain decoupled pairs of equations. As a result, $\hat{a}_{1-} = \hat{a}_{2+} = 0$ can be used as the first approximation. The remaining two equations involving $\hat{a}_{1+}$ and $\hat{a}_{2-}$ are made into standard form by introducing the transformation

$$Y = \hat{a}_{1+} + \hat{a}_{2-}$$

$$y = \hat{a}_{1+} - \hat{a}_{2-}$$

and changing them into two second-order equations. The

equivalent second-order equations are

$$Y'' - \frac{[\beta(1+k)]'}{\beta(1+k)} Y' + \beta^2(1-k^2)Y = 0 \qquad \text{(A2a)}$$

$$y'' - \frac{[\beta(1-k)]'}{\beta(1-k)} y' + \beta^2(1-k^2)y = 0. \qquad \text{(A2b)}$$

Since it is not of our concern, we omit the details of physical optics approximation and simply give the solution here. The reader is referred to standard text books, e.g. [23]. The final form of $\hat{a}_{1+}$ and $\hat{a}_{2-}$ are given by

$$\hat{a}_{1+} = \frac{1}{j\omega\sqrt{2Z_s}} \left\{ \frac{(1-k^2(0))^{1/4}\left(\sqrt{1+k(x)} + \sqrt{1-k(x)}\right)}{\left(\sqrt{1+k(0)} + \sqrt{1-k(0)}\right)(1-k^2(x))^{1/4}} \cdot \frac{e^{-js(x)}}{1-R(0)R(l)e^{-2js(l)}} \right.$$

$$\left. + \frac{(1-k^2(0))^{1/4}\left(\sqrt{1-k(x)} - \sqrt{1+k(x)}\right)}{\left(\sqrt{1+k(0)} + \sqrt{1-k(0)}\right)(1-k^2(x))^{1/4}} \cdot \frac{R(l)e^{js(x)-2js(l)}}{1-R(0)R(l)e^{-2js(l)}} \right\} \qquad \text{(A3a)}$$

$$\hat{a}_{2-} = \frac{1}{j\omega\sqrt{2Z_s}} \left\{ \frac{(1-k^2(0))^{1/4}\left(\sqrt{1-k(x)} - \sqrt{1+k(x)}\right)}{\left(\sqrt{1+k(0)} + \sqrt{1-k(0)}\right)(1-k^2(x))^{1/4}} \cdot \frac{e^{-js(x)}}{1-R(0)R(l)e^{-2js(l)}} \right.$$

$$\left. + \frac{(1-k^2(0))^{1/4}\left(\sqrt{1-k(x)} + \sqrt{1+k(x)}\right)}{\left(\sqrt{1+k(0)} + \sqrt{1-k(0)}\right)(1-k^2(x))^{1/4}} \cdot \frac{R(l)e^{js(x)-2js(l)}}{1-R(0)R(l)e^{-2js(l)}} \right\} \qquad \text{(A3b)}$$

where $s(x) = \omega x / c_0$.

In both expressions, we identify the term containing $e^{-js(x)}$ as the forward propagating mode, while the one containing $e^{js(x)}$ as the backward propagating mode. Additional information is obtained by expanding the term

$$\frac{1}{1-R(0)R(l)e^{-2js(l)}} = \sum_{n=0}^{\infty} [R(0)R(l)]^n e^{-2jns(l)}.$$

Thus, after transforming back to time domain, we find that the physical optics approximation reproduces the zeroth-order terms.

## References


[1] J. R. Pierce, "Coupling of modes of propagation," *J. Appl. Phys.*, vol. 25, pp. 179–183, Feb. 1954.

[2] E. M. T. Jones and J. T. Bolljahn, "Coupled-strip-transmission-line filters and directional couplers," *IRE Trans. Microwave Theory Tech.*, vol. MTT-4, pp. 75–81, Apr. 1956.

[3] C. C. Johnson, *Field and Wave Electrodynamics*. New York: McGraw-Hill, 1966.

[4] V. Dvorak, "Numerical solution of the transient response of a distributed parameter transformer," *IEEE Trans. Circuit Theory*, vol. CT-18, pp. 270–273, May 1970.

[5] H. W. Dommel, "Digital computer solutions of electromagnetic transients in single and multiphase networks," *IEEE Trans. Power App. Syst.*, vol. PAS-88, pp. 388–399, Apr. 1969.

[6] S. J. Garrett, "Transmission line models for transient analysis," in *Proc. 11th Design Automation Workshop* (Denver, CO), June 1974, pp. 209–219.

[7] S. Bernstein, "Transmission line models, a unified physical network approach," in *Proc. 13th Design Automation Workshop* (San Francisco, CA), June 1976, pp. 117–130.

[8] P. M. Grau, "The effect of crossing lines on electrical parameters of multi-conductor printed circuit hardware," in *Conf. Rec., 12th Asilomar Conf. Circuits Systems & Computers*, Nov. 1978, pp. 516–520.

[9] J. Chilo and T. Arnaud, "Coupling effects in the time domain for an interconnecting bus in high-speed GaAs logic circuits," *IEEE Trans. Electronic Devices*, vol. ED-31, pp. 347–352, Mar. 1984.

[10] E. Weber, *Linear Transient Analysis*, vol. II. New York: Wiley, 1956.

[11] C. T. Tai, "Transients on lossless terminated transmission lines," *IEEE Trans. Antennas Propagat.*, vol. AP-26, pp. 556–561, July 1978.

[12] C. W. Barnes, "On the impulse response of a coupled-mode system," *IEEE Trans. Microwave Theory Tech.*, vol. MTT-13, pp. 432–435, July 1965.

[13] A. H. Mohammadian and C. T. Tai, "Transients on lossy transmission lines with arbitrary boundary conditions," *IEEE Trans. Antennas Propagat.*, vol. AP-32, pp. 418–422, Apr. 1984.

[14] C. Cases and D. M. Quinn, "Transient response of uniformly distributed RLC transmission lines," *IEEE Trans. Circuits Syst.*, vol. CAS-27, pp. 200–207, Mar. 1980.

[15] A. J. Gruodis and C. S. Chang, "Coupled lossy transmission line characterization and simulation," *IBM J. Res. Develop.*, vol. 25, pp. 25–41, Jan. 1981.

[16] F. H. Branin, Jr., "Transient analysis of lossless transmission lines," *Proc. IEEE*, vol. 55, pp. 2012–2013, Nov. 1967.

[17] F. Y. Chang, "Transient analysis lossless coupled transmission lines in a nonhomogeneous medium," *IEEE Trans. Microwave Theory Tech.*, vol. MTT-18, pp. 616–626, Sept. 1970.

[18] V. Dvorak, "Computer simulation of signal propagation through a nonuniform transmission line," *IEEE Trans. Circuit Theory*, vol. CT-20, pp. 580–583, Sept. 1973.

[19] J. E. Adair and G. I. Haddad, "Coupled-mode analysis of nonuniform coupled transmission lines," *IEEE Trans. Microwave Theory Tech.*, vol. MTT-17, pp. 746–752, Oct. 1969.

[20] R. Courant and D. Hilbert, *Methods of Mathematical Physics*, vol. II. New York: Wiley-Interscience, 1962.

[21] A. H. Mohammadian and C. T. Tai, "A general method of transient analysis for lossless transmission lines and its analytical solution to time-varying resistive terminations," *IEEE Trans. Antennas Propagat.*, vol. AP-32, pp. 309–312, Mar. 1984.

[22] M. Abourzahra and L. Lewin, "Theory and application of coupling between curved transmission lines," *IEEE Trans. Microwave Theory Tech.*, vol. MTT-30, pp. 1988–1995, Nov. 1982.

[23] C. M. Bender and S. A. Orszag, *Advanced Mathematical Methods for Scientists and Engineers*. New York: McGraw-Hill, 1978.


✠

**Ying-ching Eric Yang** (S'84) was born in Taichung, Taiwan, Republic of China on May 14, 1959. He received the B.S.E.E. degree from

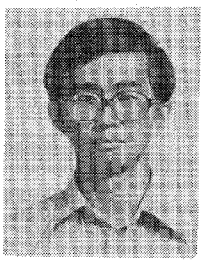

National Taiwan University, Taipei, in 1981, and the M.S. degree in electrical engineering from the Massachusetts Institute of Technology, Cambridge, in 1985. He is currently working toward the Ph.D. degree.

From 1981 to 1983, he served in the Chinese Navy as an Instructor. Since 1983, he has been with the Department of Electrical Engineering and Computer Science and the Research Laboratory of Electronics of the Massachusetts Institute of Technology, where he worked as a Research Assistant and a Teaching Assistant. His research interest is in the time-domain and frequency-domain analysis of electromagnetic-wave propagation in layered media.

✠

**Jin Au Kong** (S'65–M'69–SM'74–F'85) is a Professor of Electrical Engineering at the Massachusetts Institute of Technology in Cambridge, MA. From 1977–1980, he served the United Nations as a High-level Consultant to the Under-Secretary-General on science and technology, and as an Interregional Advisor on remote sensing technology for the Department of Technical Cooperation for Development. he was an External Examiner for the Electronics Department of the Chinese University of Hong Kong (1981–1983), and an IEEE Antennas and Propagation Society Distinguished Lecturer (1982–1984).

His research interests are in the area of electromagnetic-wave propagation, scattering, and radiation with applications to microwave remote sensing, geophysical exploration, and electromagnetic transmission and coupling in microelectronic integrated circuits. He has published four books, over 100 refereed journal articles, and 70 conference papers, and supervised over 70 theses. He is currently the editor for the Wiley series in remote sensing. In 1985, he received the Excellence in Teaching Award from the graduate student council at MIT.

✠

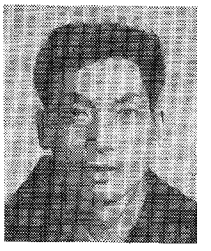

**Qizheng Gu** was born in Jiangsu, China. He received the B.S. degree from Fudan University, Shanghai, in 1960.

From 1960 to 1962, he worked on the design and analysis of automatic control systems at Shanghai Designing Institute of Machinery and Electrical Engineering, China. In 1962, he joined the Department for Research and Development at Shanghai Xinhua Radio Factory, where he was engaged in research on microwave passive and active devices, receiver systems, PLL and AFC systems, and microwave integrated circuits. Since October 1982, he has been a senior engineer and the Deputy Director of the Department for Research and Development. In June 1983, he came to the Massachusetts Institute of Technology as a Visiting Scientist at the Research Laboratory of Electronics.

Mr. Gu is a member of Shanghai Electronics Association Council and the Microwave Committee of the Chinese Institute of Electronics.